

Early Black Holes in Cosmological Simulations: Luminosity Functions and Clustering Behaviour

Colin DeGraf¹, Tiziana Di Matteo¹, Nishikanta Khandai¹, Rupert Croft¹,
Julio Lopez², Volker Springel^{3,4}

¹ *McWilliams Center for Cosmology, Carnegie Mellon University, 5000 Forbes Avenue, Pittsburgh, PA 15213, USA*

² *Computer Science Department, Carnegie Mellon University, 5000 Forbes Avenue, Pittsburgh PA 15213, USA*

³ *Heidelberg Institute for Theoretical Studies, Schloss-Wolfsbrunnengasse 35, 68118 Heidelberg, Germany*

⁴ *Zentrum für Astronomie der Universität Heidelberg, Astronomisches Recheninstitut, Mönchhofstr. 12-14, 69120 Heidelberg, Germany*

Accepted 20?? ???? ?. Received 20?? ???? ??. in original form 20?? xx

ABSTRACT

We examine predictions for the quasar luminosity functions (QLF) and quasar clustering at high redshift ($z \geq 4.75$) using *MassiveBlack*, our new hydrodynamic cosmological simulation which includes a self-consistent model for black hole growth and feedback. We show that the model reproduces the Sloan QLF within observational constraints at $z \geq 5$. We find that the high- z QLF is consistent with a redshift-independent occupation distribution of BHs among dark matter halos (which we provide) such that the evolution of the QLF follows that of the halo mass function. The sole exception is the bright-end at $z = 6$ and 7 , where BHs in high-mass halos tend to be unusually bright due to extended periods of Eddington growth caused by high density cold flows into the halo center. We further use these luminosity functions to make predictions for the number density of quasars in upcoming surveys, predicting there should be $\sim 119 \pm 28$ ($\sim 87 \pm 28$) quasars detectable in the F125W band of the WIDE (DEEP) fields of the Cosmic Assembly Near-infrared Deep Extragalactic Legacy Survey (CANDELS) from $z = 5 - 6$, $\sim 19 \pm 7$ ($\sim 18 \pm 9$) from $z = 6 - 7$, and $\sim 1.7 \pm 1.5$ ($\sim 1.5 \pm 1.5$) from $z = 7 - 8$. We also investigate quasar clustering, finding that the correlation length is fully consistent with current constraints for Sloan quasars ($r_0 \sim 17 h^{-1}$ Mpc at $z = 4$ for quasars above $m_i = 20.2$), and grows slowly with redshift up to $z = 6$ ($r_0 \sim 22 h^{-1}$ Mpc). Finally, we note that the quasar clustering strength depends weakly on luminosity for low L_{BH} , but gets stronger at higher L_{BH} as the BHs are found in higher mass halos.

Key words: quasars: general — galaxies: active — black hole physics — methods: numerical — galaxies: haloes

1 INTRODUCTION

Supermassive black holes are believed to be present at the center of most galaxies (Kormendy & Richstone 1995) and are found to be correlated with the properties of their host galaxies (Magorrian et al. 1998; Ferrarese & Merritt 2000; Gebhardt et al. 2000; Tremaine et al. 2002; Graham & Driver 2007). These correlations provide strong evidence for a link between the growth of black holes and the evolution of their host galaxies, generally attributed to some form of quasar feedback (Burkert & Silk 2001; Granato et al. 2004; Sazonov et al. 2004; Springel et al. 2005b; Churazov et al. 2005; Kawata & Gibson 2005; Di Matteo et al. 2005; Bower et al. 2006; Begelman et al. 2006; Croton et al. 2006;

Malbon et al. 2007; Ciotti & Ostriker 2007; Sijacki et al. 2007; Hopkins et al. 2007).

Perhaps the most fundamental statistical quantity in the study of quasars is the number density, often characterized as a Quasar Luminosity Function (QLF). The QLF has been studied observationally (La Franca et al. 2002; Fiore et al. 2003; Ueda et al. 2003; Barger et al. 2003b; Croom et al. 2004; La Franca et al. 2005; Cirasuolo et al. 2005; Richards et al. 2006; Brown et al. 2006; Silverman et al. 2008; Ebrero et al. 2009; Yenko et al. 2009), as well as through simulations, with black holes modeled both semi-analytically (Kauffmann & Haehnelt 2000; Volonteri et al. 2003; Wyithe & Loeb 2003; Granato et al. 2004; Marulli et al. 2008; Bonoli et al. 2009) and directly incorporated in the

simulation (Hopkins et al. 2005b, 2006b, 2007; Marulli et al. 2009; DeGraf et al. 2010).

Another fundamental quantity for quasar populations is the strength of quasar clustering, and its evolution with redshift. Numerous observational studies have been done (La Franca et al. 1998; Porciani et al. 2004; Croom et al. 2005; Shen et al. 2007; Myers et al. 2007; da Ángela et al. 2008; Shen et al. 2009; Ross et al. 2009), generally finding evidence for increasing clustering amplitude with redshift, in agreement with findings from simulations (Bonoli et al. 2009; Croton 2009; DeGraf et al. 2010). Clustering is especially significant because one can use it to estimate the typical dark matter halos in which quasars are found simply by comparing the clustering strength of quasars to that of dark matter halos. In particular, the luminosity dependence of the clustering (if any) can help determine if the bright and faint quasars populate the same halos, suggesting they may be the same population of quasars at different phases of their lives (see, e.g. Hopkins et al. 2005b,d,c,a, 2006a) or different halo masses, suggesting they are fundamentally different quasar populations (see, e.g. Lidz et al. 2006).

Thus both QLF and quasar clustering can be used to investigate the populations of quasars being observed, how they populate dark matter halos, and how the typical luminosities correlate with hosts. However, investigations at high redshift have been extremely difficult. Simulations have proved difficult due to the volumes needed to produce high redshift quasars in sufficient numbers, limiting the statistical investigations. Similarly, the difficulty observing such distant objects limits the current number of observed high redshift quasars such that the $z \sim 6$ faint-end QLF is determined by only a few objects (Willott et al. 2010b), and high-redshift quasar clustering is limited to lower redshift (e.g. $z \sim 4$ by Shen et al. 2009). However, upcoming surveys such as the James Webb Space Telescope (JWST) and the Cosmic Assembly Near-infrared Deep Extragalactic Legacy Survey (CANDELS) have the potential to drastically improve the high- z observations, making now an ideal time to make predictions as to the statistics of high redshift quasars.

In this paper we use a new large-scale hydrodynamic cosmological simulation to study the earliest supermassive black holes, focusing on their luminosity and clustering properties. We take advantage of this simulation’s large volume (it is the largest cosmological simulation which directly models the growth and evolution of black holes) to investigate the statistical properties of the earliest supermassive black holes, focusing on the luminosity function and correlation length. We use these quantities to compare with current observational measurements, to make predictions for upcoming surveys, and to investigate the implications of potential features which may be detected.

In Section 2 we describe the numerical simulation used for our analysis. In Section 3 we investigate the Quasar Luminosity Function (Section 3.1) and quasar clustering (Section 3.2) and compare with observations, and our results are summarized in Section 4.

2 METHOD

In this paper we use a new cosmological hydrodynamic simulation of a $533 h^{-1}$ Mpc box specifically intended

Table 1. Numerical Parameters

Boxsize h^{-1} Mpc	N_p	m_{DM} $h^{-1}M_\odot$	m_{gas} $h^{-1}M_\odot$	ϵ h^{-1} kpc
533.33	2×3200^3	$2.8 \times 10^8 M_\odot$	$5.7 \times 10^7 M_\odot$	5.0

for high-redshift investigations (see Table 1). The simulation uses the massively parallel cosmological TreePM-SPH code GADGET-3 (an updated version of GADGET-2, see Springel 2005) incorporating a multi-phase ISM model with star formation (Springel & Hernquist 2003) and black hole accretion and feedback (Springel et al. 2005a; Di Matteo et al. 2005).

Within our simulation, black holes are modeled as collisionless sink particles which form in newly emerging and resolved dark matter halos. These halos are found by calling a friends of friends group finder at regular intervals (in time intervals spaced by $\Delta \log a = \log 1.25$). Any group above a threshold mass of $5 \times 10^{10} h^{-1} M_\odot$ not already containing a black hole is provided one by converting its densest particle to a sink particle with a seed mass of $M_{BH,seed} = 5 \times 10^5 h^{-1} M_\odot$. This seeding prescription is chosen to reasonably match the expected formation of supermassive black holes by gas directly collapsing to BHs with $M_{BH} \sim M_{seed}$ (e.g. Bromm & Loeb 2003; Begelman et al. 2006) or by PopIII stars collapsing to $\sim 10^2 M_\odot$ BHs at $z \sim 30$ (Bromm & Larson 2004; Yoshida et al. 2006) followed by sufficient exponential growth to reach M_{seed} by the time the host halo reaches $\sim 10^{10} M_\odot$. Following insertion, BHs grow in mass by accretion of surrounding gas and by merging with other black holes. Gas is accreted according to $\dot{M}_{BH} = \alpha \frac{4\pi G^2 M_{BH}^2 \rho}{(c_s^2 + v^2)^{3/2}}$ (Hoyle & Lyttleton 1939; Bondi & Hoyle 1944; Bondi 1952), where ρ is the local gas density, c_s is the local sound speed, v is the velocity of the BH relative to the surrounding gas, and α is introduced to correct for the reduction of the gas density close to the BH due to our effective sub-resolution model for the ISM. To allow for the initial rapid BH growth necessary to produce sufficiently massive BHs at early time ($\sim 10^9 M_\odot$ by $z \sim 6$) we allow for mildly super-Eddington accretion (consistent with Volonteri & Rees 2006; Begelman et al. 2006), but limit it to a maximum of $3 \times \dot{M}_{Edd}$ to prevent artificially high values.

The BH is assumed to radiate with a bolometric luminosity proportional to the accretion rate, $L = \eta \dot{M}_{BH} c^2$ (Shakura & Sunyaev 1973), where the radiative efficiency η is fixed to 0.1 throughout the simulation and our analysis. To model the expected coupling between the liberated radiation and the surrounding gas, 5 per cent of the luminosity is isotropically deposited to the local black hole kernel as thermal energy. The 5 per cent value for the coupling factor is based on galaxy merger simulations such that the normalization of the $M_{BH} - \sigma$ relation is reproduced (Di Matteo et al. 2005).

The second mode of black hole growth is through mergers which occur when dark matter halos merge into a single halo, such that their black holes fall toward the center of the new halo, eventually merging with one another. In cosmological volumes, it is not possible to directly model the physics of the infalling BHs at the smallest scales, so a sub-

resolution model is used. Since the mergers typically occur at the center of a galaxy (i.e. a gas-rich environment), we assume the final coalescence will be rapid (Makino & Funato 2004; Escala et al. 2004; Mayer et al. 2007), so we merge the BHs once they are within the spatial resolution of the simulation. However, to prevent merging of BHs which are rapidly passing one another, mergers are prevented if the BHs' velocity relative to one another is too high (comparable to the local sound speed).

The model used for black hole creation, accretion and feedback has been investigated and discussed in Sijacki et al. (2007); Di Matteo et al. (2008); Colberg & di Matteo (2008); Croft et al. (2009); Sijacki et al. (2009); DeGraf et al. (2010); Degraf et al. (2011), finding it does a good job reproducing the $M_{\text{BH}} - \sigma$ relation, the total black hole mass density (Di Matteo et al. 2008), the QLF (DeGraf et al. 2010), and the expected black hole clustering behavior (Degraf et al. 2011). This simple model thus appears to model the growth, activity, and evolution of supermassive black holes in a cosmological context surprisingly well (though the detailed treatment of the accretion physics is infeasible for cosmological scale simulations). We also note that Booth & Schaye (2009) and Johansson et al. (2008) have adopted a very similar model, and have independently investigated the parameter space of the reference model of Di Matteo et al. (2008), as well as varying some of the underlying prescriptions. For further details on the simulation methods and convergence studies done for similar simulations, see Di Matteo et al. (2008).

Because the simulation saves the complete set of black hole properties (mass, accretion rate, position, local gas density, sound speed, velocity, and BH velocity relative to local gas) for each BH at every timestep, the black hole output for such a large simulation is prohibitively difficult to analyze using previous techniques. For this reason, Lopez et al. (2011) developed a relational database management system specifically for this simulation. A similar strategy has also been followed in the analysis of the Millenium simulation (Lemson & Virgo Consortium 2006). In addition to providing a substantially more efficient query system for extracting information, this database is significantly more flexible than traditional approaches. For a complete summary of the database format and its efficiency, please see Lopez et al. (2011).

3 RESULTS

3.1 Luminosity Function

In the left panel of Figure 1 we show the bolometric Quasar Luminosity Function for $L_{\text{BH}} > 10^{10} L_{\odot}$ at $z = 11$ to $z = 5$ (solid lines). We also show the observational data compiled by Willott et al. (2010a) from SDSS main (diamonds, Fan et al. 2006), SDSS deep stripe (triangles, Jiang et al. 2009), and the Canda-France High- z Quasar Survey (circles, Willott et al. 2010b), and that compiled by Hopkins et al. (2007) (asterisks; Fan et al. 2001b,a; Barger et al. 2003b,a; Fan et al. 2003, 2004; Cristiani et al. 2004; Barger et al. 2005; Richards et al. 2005; Silverman et al. 2005). We find that our simulation is generally consistent with observations, though we tend to predict a steeper slope than observations.

Thus this large simulation volume shows that our model is capable of producing Sloan-type BHs at high redshift ($z = 5, 6$), and in the correct abundances (and in fact of sufficiently high mass, see Di Matteo et al. 2011).

To help better understand the quasar populations which we are simulating and the dark matter halos in which they are found, we have performed a simple fit to characterize the relation between BH luminosity and host halo mass. To do this, we use a simple Halo Occupation Distribution (HOD) model. Because we are only interested in the high-luminosity sources (and it is exceedingly rare to find multiple high-luminosity objects within a single halo, especially at such high redshift), we model the probability that a halo of a given mass (M_{Host}) will host a BH above a specified luminosity ($L_{\text{BH,cut}}$) as a cumulative log-normal distribution (which is often used in galaxy HOD models for $\langle N_{\text{cen}} \rangle$, see, e.g. Zheng et al. 2005)

$$f(L_{\text{BH,cut}}|M_{\text{Host}}) = \frac{1}{2} \left(1 + \text{erf} \left(\frac{\ln(M_{\text{Host}}) - \mu(L_{\text{BH,cut}})}{\sqrt{2\sigma^2(L_{\text{BH,cut}})}} \right) \right) \quad (1)$$

where $f(L_{\text{BH,cut}}|M_{\text{Host}})$ is the fraction of halos with mass M_{Host} which contain a BH above $L_{\text{BH,cut}}$, and erf is the error function ($\text{erf}(x) = \frac{2}{\sqrt{\pi}} \int_0^x e^{-y^2} dy$) [see Table 2 for fitted parameters]. We combine this occupation fraction (using parameters at $z = 5$) with the halo mass function of Reed et al. (2007) to predict the QLF, shown in Figure 1 (blue dashed line). This predicted QLF matches the simulation well at $z = 5$, confirming an accurate fit. We note that our HOD approach may slightly underpredict the low luminosities since the HOD parameters are fit for bright ($> 10^{11} L_{\odot}$) quasars, and because at low luminosities, satellite BHs (which are not included in our simple HOD) may become significant. For bright objects, however, this approach is very accurate.

We also plot the QLF for higher redshifts using the $z = 5$ HOD fit (dashed lines), and find that it does a surprisingly good job of predicting the higher redshift QLF, with the exception of the luminous BHs at $z = 6$ and 7. This suggests that the manner in which BHs populate halos is approximately redshift independent, save for the luminous BHs at redshifts 6 and 7. At these redshifts, we find the rarest (i.e. brightest) objects to be brighter than our $z = 5$ fit would expect. In other words, at $z = 6$ and 7, the BHs in the most massive halos are more luminous than those in comparable halos at other redshifts, a result of unusually high accretion rates. To quantify this discrepancy, we performed HOD fits for $z = 6, 7$ (Table 2) which are shown as dotted lines in Figure 1. We note that A_{μ} remains approximately constant, suggesting that BHs of $\sim 10^{11} L_{\odot}$ tend to populate similar-size halos regardless of redshift (at least for $z \geq 5$). However, at $z = 6$ and 7 the smaller B_{μ} implies that BHs found in massive halos at $z = 6$ and 7 tend to be brighter than those in comparable halos at other redshifts, and the effect gets stronger for higher mass halos/higher luminosity BHs.

This can be explained by considering the growth history of the massive BHs. Di Matteo et al. (2011) find that the most massive BHs typically undergo a period of rapid (i.e. Eddington) growth in this general redshift range ($z \sim 6 - 8$) as a result of high density streams of cold gas which not only help assemble the first massive halos, but appear to

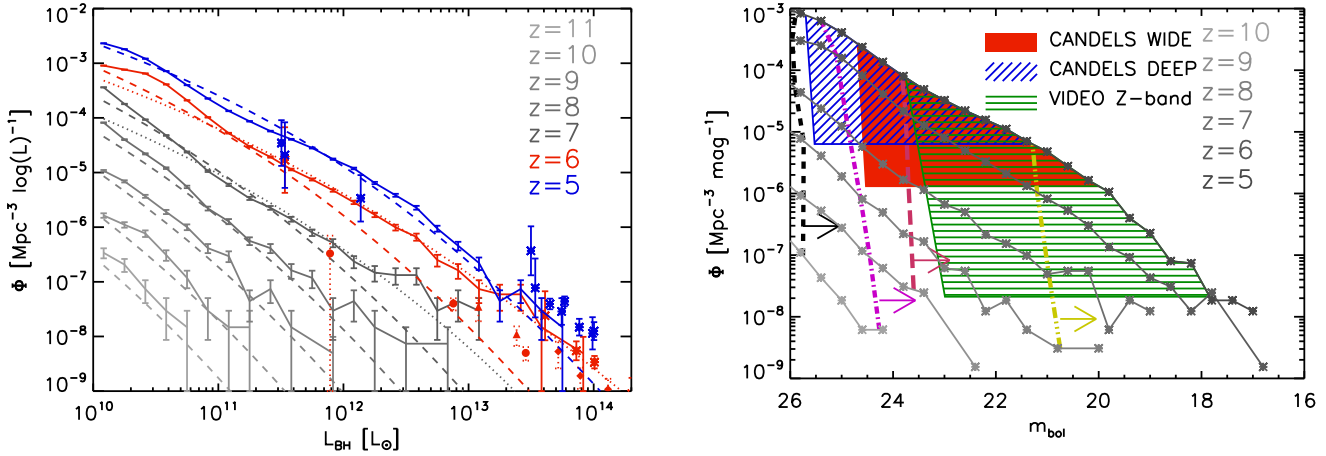


Figure 1. *Left panel:* Quasar luminosity function for $z = 11$ to $z = 5$ (solid lines with Poisson error bars), along with the $z = 5$ and 6 observational datapoints compiled by Willott et al. (2010a) and Hopkins et al. (2007) [See text for complete references to observational data]. We also show the predicted QLF from our HOD model using the $z = 5$ fit (dashed lines) and using redshift-specific fits (dotted lines). [See Table 2 for fitted parameters.] *Right panel:* Quasar magnitude function for $z = 11$ to $z = 5$, based on apparent bolometric magnitude. The regions probed by CANDELS and VIDEO surveys are shown as shaded regions (solid red - CANDELS DEEP; hatched blue - CANDELS WIDE; hatched green - VIDEO). The lower limits are based on the survey volume for $z \pm 0.5$. We also show the magnitude limits for JWST NIRCAM (black dashed), LSST (pink dot-dashed), Dark Energy Survey (red long dashed), and VIKING (yellow triple-dot dash).

penetrate to the halo centers. These cold flows facilitate extended periods of Eddington growth of BHs in the most massive halos, which manifests itself in the QLF by flattening the bright end. This continues until the energy released by the quasar heats the surrounding gas to such a point that it is blown away from the halo center, and the BHs become self-regulated (see Di Matteo et al. 2011, for an investigation into this behavior), at which point the bright-end will steepen once again. In this picture, the QLF should roughly follow the evolution of the halo mass function except for those BHs undergoing their Eddington growth phase, where the luminosity should be unusually high. We find exactly these results in Figure 1, where the $z = 5$ fit does a good job except in the bright-end at $z = 6 - 7$, where Eddington growth is common.

In addition to the luminosity function shown in the left panel of Figure 1, we show the magnitude function in terms of apparent bolometric magnitude in the right panel which we use as a basis for predictions for several upcoming surveys. In particular, we show the regimes probed by the Cosmic Assembly Near-IR Deep Extragalactic Legacy Survey (CANDELS) WIDE and DEEP surveys¹ (solid red and hatched blue, respectively). These regions are bounded by the magnitude limit of the F125W filter (converted to bolometric magnitude using the spectral energy distribution (SED) of Hopkins et al. 2007), and the volume enclosed by the survey areas ($m < 26.4$ over 0.2 deg^2 for WIDE and $m < 27.4$ over 0.04 deg^2 for DEEP, assuming a redshift range of ± 0.5). We predict that both the WIDE and DEEP programs will find sources out to $z \sim 7 - 8$, with each probing a slightly different region of the luminosity function. We expect there to be $\sim 119 \pm 28$ ($\sim 87 \pm 28$) quasars bright enough in the F125W band of the CAN-

DELS WIDE (DEEP) fields from $z = 5 - 6$, $\sim 19 \pm 7$ ($\sim 18 \pm 9$) from $z = 6 - 7$, and $\sim 1.7 \pm 1.5$ ($\sim 1.5 \pm 1.5$) from $z = 7 - 8$. This will drastically increase the number of high-redshift quasars, which will substantially improve the measurements of the faint end of the $z = 6$ QLF, and the different (though overlapping) ranges probed by the WIDE and DEEP programs will help constrain the faint-end slope. We have also provided a similar bounded volume for the VISTA Deep Extragalactic Observations Survey (VIDEO), and magnitude limits for JWST’s Near-Infrared Camera (NIRCAM; black dashed line) (Gardner et al. 2006), Large Synoptic Survey Telescope (LSST; pink dot-dashed), Dark Energy Survey (red long dashed), and VISTA Kilo-Degree IR Galaxy Survey (VIKING; yellow triple-dot dash), each converted to bolometric magnitudes (using the SED of Hopkins et al. 2007) to provide the means for predicting the number of high- z quasars these surveys should find. Overall, these surveys should drastically improve the measurements of the faint-end QLF by improving the number of observed quasars, and pushing to luminosities an order of magnitude lower than current observations.

3.2 Quasar Clustering

In addition to the number density of quasars, we look at the clustering properties characterized by the correlation length (r_0 , defined as the scale at which the correlation function $\xi(r_0) = 1$). In Figure 2 we show the predicted correlation length as a function of lower-luminosity cut for $z = 1$ to 6 . These predicted correlation lengths are obtained using a halo mass function (Reed et al. 2007) and the halo bias factor of Sheth et al. (2001), weighted by the fraction of halos hosting sufficiently luminous quasars (Eqn. 1, using the $z = 5$ parameters for $z \leq 5$ and the $z = 6$ fit at $z = 6$). We note that the halo bias factor is not well constrained for the very high-mass end (see, e.g. Tinker et al. 2010; Pillepich et al. 2010),

¹ <http://candels.ucolick.org>

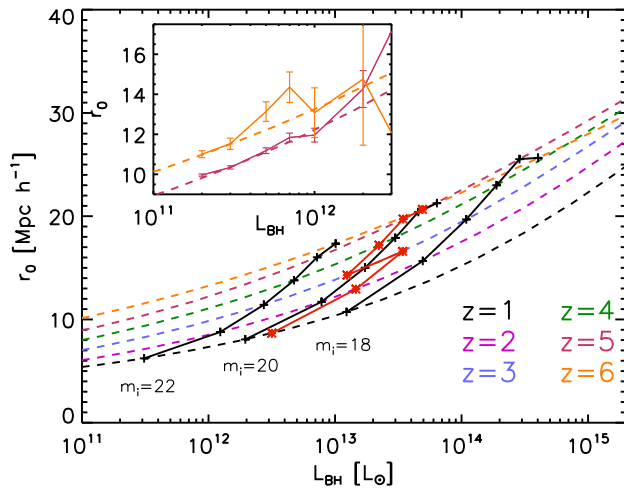


Figure 2. *Main panel:* The predicted correlation length based on our HOD model as a function of luminosity (dashed lines). Curves of constant apparent i-band magnitude are shown in black, and the magnitude cut used for quasars by SDSS (19.1 for $z < 3$, 20.2 for $z > 3$) is shown in red. Note that the $z < 5$ curves use the $z = 5$ HOD fit. *Inset:* Comparison of r_0 from the HOD-based prediction (dashed lines) and that obtained directly from our simulation (solid lines) for $z = 5$ (red) and 6 (orange).

and has not been investigated significantly at these high redshifts. Nonetheless, we find that the Sheth et al. (2001) bias factor does a good job of modeling our halo bias, though at $z \sim 6$ it underestimates by $\sim 5\%$ relative to our simulation (note that we adjustment the bias factor by 5% to account for this when calculating $r_{0,\text{BH}}$). This technique is important as it allows us to extend our predictions to higher luminosities where we do not have sufficient BHs to obtain clustering statistics.

To confirm the validity of this approach, we calculate the correlation length directly from the simulation using a maximum likelihood estimator (see, e.g. Croft et al. 1997), and show the comparison in the inset plot (dashed lines - HOD model; solid lines - direct from simulation), finding good agreement in the luminosity range probed directly by our simulation. Thus we confirm that the large-scale clustering of luminous quasars can be well-modeled by the clustering of dark matter halos and a relatively simple BH HOD (Eqn. 1). In the main plot we also show curves of constant apparent magnitude (solid black curves), and a curve for the magnitude cut used for quasar selection in SDSS ($m_i < 20.2$ for $z > 3$, $m_i < 19.1$ for $z < 3$, solid red curve). These curves show that using a magnitude cut rather than a luminosity cut will increase the observed redshift evolution. We also see that the evolution of the clustering strength with luminosity is relatively minor for low- L_{BH} (where BHs occupy the slowly-evolving end of the halo mass function), but becomes more significant at high luminosities where BHs occupy the high-mass tail of the mass function.

In addition, we note the effect of the change in the HOD model from $z = 5$ (red) to $z = 6$ (orange). For low luminosities (below $\sim 10^{13} L_{\odot}$) there is minimal effect, due to the similarity in A_{μ} . However, the smaller B_{μ} at $z = 6$ (Table 2) means that higher luminosity BHs will typically be found in smaller halos, which have a correspondingly lower

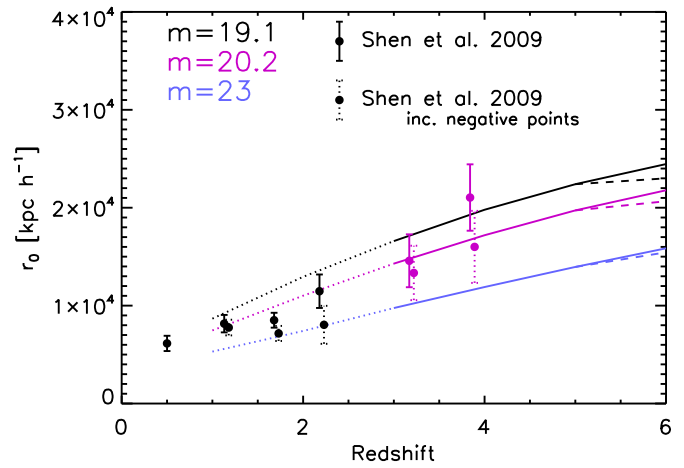


Figure 3. Evolution in the predicted correlation length assuming a redshift independent HOD fit (using $z = 5$ parameters) for magnitude cuts of 19.1 (black, SDSS QSO cut for $z < 3$), 20.2 (pink, SDSS QSO cut for $z > 3$), and 23.0 (blue). The dashed line from $z = 5$ to 6 shows r_0 if $z = 6$ HOD fit is used at $z = 6$. *Filled circles:* Observational data from Shen et al. (2009) obtained with and without negative datapoints (dashed and solid error bars, respectively).

correlation length. Because the effect grows with luminosity, the difference manifests itself in the shallower slope of r_0 vs. L_{BH} , even resulting in a crossover at $\sim 4 \times 10^{13} L_{\odot}$. We note that this crossover is highly dependent on the HOD at high luminosities, and we are forced to extrapolate our HOD to reach these values. Thus this crossover is not a strong prediction (see further discussion below) but the general suppression is a clear trend in our simulation. In this way we see that r_0 could be effected by a change in the HOD, but the effect should be fairly minor and will only occur at extremely high luminosities ($\gtrsim 10^{13.5} L_{\odot}$).

In Figure 3 we show the evolution in our predicted correlation length for SDSS-type quasars based on our $z = 5$ HOD fit (for luminosity cuts corresponding to $m_i < 19.1$ - Black; $m_i < 20.2$ - Pink; $m_i < 23.0$ - Blue), together with the observed measurements of Shen et al. (2009) (obtained with and without inclusion of negative datapoints, shown with dashed and solid error bars respectively). The curves assume constant occupation behavior (i.e. the $z = 5$ HOD parameters are used at all redshifts). Based on earlier work, we would expect relatively minor evolution in the HOD between $z = 5$ and $z = 3$ (Chatterjee et al. 2011), so the extrapolation should remain fairly accurate for $z > 3$. This extrapolation shows that our simulation is able to reproduce the large correlation lengths ($r_0 \sim 17 h^{-1}$ Mpc at $z = 4$) from observational constraints. In addition, we match the rough evolution with redshift for $z > 3$, and we expect r_0 to continue to increase with redshift, reaching $\sim 22 h^{-1}$ Mpc by $z = 6$. Because we use a redshift-independent BH HOD model, this agreement with the observed evolution of r_0 with redshift suggests that high- z quasar clustering evolution can be completely explained by the evolution in the clustering of dark matter halos, i.e. without evolution in the mass of the typical host halo. Below $z = 3$ we expect the AGN HOD to evolve more quickly (Chatterjee et al. 2011), so the extrap-

Table 2. Luminosity dependence of μ and σ (see Eqn. 1).

$$\mu, \sigma(L_{\text{BH,cut}}) = A_{\mu,\sigma} \times \left(\frac{L_{\text{BH,cut}}}{10^{11} L_{\odot}} \right)^{B_{\mu,\sigma}}$$

Redshift	A_{μ}	B_{μ}	A_{σ}	B_{σ}
5	27.05	.0208	.209	.128
6	26.905	.0191	.239	.133
7	27.07	.0173	.298	0

olation should not be considered an accurate prediction at lower redshifts (the dotted curves of Fig. 3), but we nonetheless appear to remain broadly consistent with observations.

In addition to the curves for the $z = 5$ HOD, we also show the effect of the change in occupation distribution from $z = 5$ to 6 (dashed lines). At $z = 6$ the shallower slope in the $L_{\text{BH}} - M_{\text{Host}}$ relation means that a given luminosity cut will correspond to a smaller typical host mass (and thereby produce a smaller r_0) at $z = 6$ than $z = 5$. Because the difference in the HOD is in the slope (B_{μ}) of the $L_{\text{BH}} - M_{\text{Host}}$ relation, the suppression gets stronger at higher luminosities and has essentially no effect on lower luminosities, which we show with the $m_i = 23.0$ curve of Figure 3. We note that the magnitude of the suppression is highly dependent on the slope of μ in Equation 1 (found in Table 2) and is only significant at luminosities above those well-probed by our simulation. As such, we cannot accurately estimate the magnitude of the suppression (or the exact luminosity at which the $z = 5$ and 6 curves of Figure 2 will cross), but we nonetheless expect a suppressed slope in the r_0 evolution from $z = 5$ to 6. Given the approximate magnitude of the suppression found in our simulation (on the order of $\sim 5\%$) and the difficulties in measuring r_0 to high precision at such high redshifts, it is unlikely that such suppression will be detected in the near future, but it is nonetheless an effect which should be considered wherever possible.

4 CONCLUSIONS

In this paper we have investigated high redshift black holes found within a new large-scale hydrodynamic simulation, focusing on the luminosity function and clustering behavior. We model the QLF for $z \geq 5$, probing black holes to luminosities up to $\sim 10^{14} L_{\odot}$. We find reasonable agreement with observational data at $z = 5$ and 6, generally falling within the variation between surveys, confirming that our model is capable of producing Sloan-type quasars at very early times as well as matching their observed abundances.

Using a HOD fit for the central AGN at $z = 5$ (which we have provided), we find that the evolution in the QLF is well described by the evolution in the halo mass function (at least for the redshifts modeled by our simulation) without significant evolution in the occupation distribution, except for the high-luminosity end at $z = 6 - 7$ where we find a significantly flatter luminosity function. We postulate this flattening of the luminosity function to be a result of the largest black holes tending to undergo unusually rapid growth (and thereby producing unusually high luminosities) during these redshifts, a conclusion supported both by the difference in the HOD fits at these redshifts, and by direct investigation into the lightcurves of these black holes

(Di Matteo et al. 2011). At lower redshift (by $z \sim 5$), self-regulation suppresses the most massive BH growth, resulting in fainter bright-end BHs, and a corresponding steepening of the QLF. In particular, we note that this increase in luminosity at $z \sim 6 - 7$ should make observations of such high- z , luminous ($> 10^{12} L_{\odot}$) BHs easier than would otherwise be expected.

We used our luminosity function to provide estimates on the number density of detectable high redshift quasars for several upcoming surveys. In particular, we expect the CANDELS survey to find quasars up to $z \sim 7$ in both the WIDE and DEEP programs, with each probing a slightly different region of the QLF. At $z \sim 6$ these programs should each detect dozens of quasars across a wide range of luminosities, drastically improving the observational constraints on the faint end of the high redshift QLF, particularly the faint-end slope. In addition, we have provided our estimated number density at each redshift for several additional upcoming surveys, thereby providing the approximate number density of quasars to be found as well as the survey areas necessary to reach the highest redshifts.

We also investigate the clustering behavior of these high redshift quasars, finding luminosity dependent correlation lengths on the order of $\sim 10 - 14 h^{-1} \text{Mpc}$. Using our HOD model and the theoretical clustering of dark matter halos, we show the correlation length as a function of BH luminosity, finding relatively weak luminosity dependence at low L_{BH} , but with increasing L_{BH} -dependence at higher luminosities (where black holes are typically found in halos in the steep end of the halo mass function). We also compare our predicted r_0 to high-redshift observations and find excellent agreement, with our simulation predicting $r_0 \sim 15 - 20 h^{-1} \text{Mpc}$ for Sloan-type quasars. We also roughly match the evolution of r_0 with redshift using a redshift-independent HOD, suggesting that high-redshift quasar clustering evolution is fully explained solely by the evolution in clustering of dark matter halos without a change in the typical host halo mass.

Finally, we note the effect a change in the BH occupation distribution from $z = 5$ to 6 has on r_0 , finding that it should suppress the clustering strength of high luminosity quasars at $z = 6$. Our limited sample size and evolution in the halo bias factor found in our simulation make it difficult to quantify the magnitude of this suppression, but we nonetheless conclude that some suppression should occur (though likely below the sensitivity of upcoming surveys).

ACKNOWLEDGMENTS

This work was supported by the National Science Foundation, NSF Petapps, OCI-0749212 and NSF AST-1009781. The simulations were carried out on Kraken at the National Institute for Computational Sciences (<http://www.nics.tennessee.edu/>).

REFERENCES

Barger A. J., et al., 2003a, AJ, 126, 632

- Barger A. J., Cowie L. L., Capak P., Alexander D. M., Bauer F. E., Brandt W. N., Garmire G. P., Hornschemeier A. E., 2003b, *ApJL*, 584, L61
- Barger A. J., Cowie L. L., Mushotzky R. F., Yang Y., Wang W.-H., Steffen A. T., Capak P., 2005, *AJ*, 129, 578
- Begelman M. C., Volonteri M., Rees M. J., 2006, *MNRAS*, 370, 289
- Bondi H., 1952, *MNRAS*, 112, 195
- Bondi H., Hoyle F., 1944, *MNRAS*, 104, 273
- Bonoli S., Marulli F., Springel V., White S. D. M., Branchini E., Moscardini L., 2009, *MNRAS*, 606
- Booth C. M., Schaye J., 2009, *MNRAS*, 398, 53
- Bower R. G., Benson A. J., Malbon R., Helly J. C., Frenk C. S., Baugh C. M., Cole S., Lacey C. G., 2006, *MNRAS*, 370, 645
- Bromm V., Larson R. B., 2004, *ARA&A*, 42, 79
- Bromm V., Loeb A., 2003, *ApJ*, 596, 34
- Brown M. J. I., et al., 2006, *ApJ*, 638, 88
- Burkert A., Silk J., 2001, *ApJL*, 554, L151
- Chatterjee S., DeGraf C., Richardson J., Zheng Z., Nagai D., Di Matteo T., 2011, *ArXiv e-prints:1104.3550*
- Churazov E., Sazonov S., Sunyaev R., Forman W., Jones C., Böhringer H., 2005, *MNRAS*, 363, L91
- Ciotti L., Ostriker J. P., 2007, *ApJ*, 665, 1038
- Cirasuolo M., Magliocchetti M., Celotti A., 2005, *MNRAS*, 357, 1267
- Colberg J. M., di Matteo T., 2008, *MNRAS*, 387, 1163
- Cristiani S., et al., 2004, *ApJL*, 600, L119
- Croft R. A. C., Dalton G. B., Efstathiou G., Sutherland W. J., Maddox S. J., 1997, *MNRAS*, 291, 305
- Croft R. A. C., Di Matteo T., Springel V., Hernquist L., 2009, *MNRAS*, 400, 43
- Croom S. M., et al., 2005, *MNRAS*, 356, 415
- Croom S. M., Smith R. J., Boyle B. J., Shanks T., Miller L., Outram P. J., Loaring N. S., 2004, *MNRAS*, 349, 1397
- Croton D. J., 2009, *MNRAS*, 394, 1109
- Croton D. J., et al., 2006, *MNRAS*, 365, 11
- da Ângela J., et al., 2008, *MNRAS*, 383, 565
- DeGraf C., Di Matteo T., Springel V., 2010, *MNRAS*, 402, 1927
- DeGraf C., Di Matteo T., Springel V., 2011, *MNRAS*, 413, 1383
- Di Matteo T., Colberg J., Springel V., Hernquist L., Sijacki D., 2008, *ApJ*, 676, 33
- Di Matteo T., Khandai N., DeGraf C., Feng Y., Croft R., Lopez J., Springel V., 2011, *ApJL* submitted
- Di Matteo T., Springel V., Hernquist L., 2005, *Nature*, 433, 604
- Ebrero J., et al., 2009, *A&A*, 493, 55
- Escala A., Larson R. B., Coppi P. S., Mardones D., 2004, *ApJ*, 607, 765
- Fan X., et al., 2004, *AJ*, 128, 515
- Fan X., et al., 2001a, *AJ*, 122, 2833
- Fan X., et al., 2006, *AJ*, 132, 117
- Fan X., et al., 2001b, *AJ*, 121, 54
- Fan X., et al., 2003, *AJ*, 125, 1649
- Ferrarese L., Merritt D., 2000, *ApJL*, 539, L9
- Fiore F., et al., 2003, *A&A*, 409, 79
- Gardner J. P., et al., 2006, *SSR*, 123, 485
- Gebhardt K., et al., 2000, *ApJL*, 539, L13
- Graham A. W., Driver S. P., 2007, *ApJ*, 655, 77
- Granato G. L., De Zotti G., Silva L., Bressan A., Danese L., 2004, *ApJ*, 600, 580
- Hopkins P. F., Hernquist L., Cox T. J., Di Matteo T., Martini P., Robertson B., Springel V., 2005a, *ApJ*, 630, 705
- Hopkins P. F., Hernquist L., Cox T. J., Di Matteo T., Robertson B., Springel V., 2005b, *ApJ*, 630, 716
- Hopkins P. F., Hernquist L., Cox T. J., Di Matteo T., Robertson B., Springel V., 2005c, *ApJ*, 632, 81
- Hopkins P. F., Hernquist L., Cox T. J., Di Matteo T., Robertson B., Springel V., 2006a, *ApJS*, 163, 1
- Hopkins P. F., Hernquist L., Cox T. J., Robertson B., Di Matteo T., Springel V., 2006b, *ApJ*, 639, 700
- Hopkins P. F., Hernquist L., Martini P., Cox T. J., Robertson B., Di Matteo T., Springel V., 2005d, *ApJL*, 625, L71
- Hopkins P. F., Richards G. T., Hernquist L., 2007, *ApJ*, 654, 731
- Hoyle F., Lyttleton R. A., 1939, in *Proceedings of the Cambridge Philosophical Society*, vol. 35 of *Proceedings of the Cambridge Philosophical Society*, 405
- Jiang L., et al., 2009, *AJ*, 138, 305
- Johansson P. H., Naab T., Burkert A., 2008, *Astronomische Nachrichten*, 329, 956
- Kauffmann G., Haehnelt M., 2000, *MNRAS*, 311, 576
- Kawata D., Gibson B. K., 2005, *MNRAS*, 358, L16
- Kormendy J., Richstone D., 1995, *ARA&A*, 33, 581
- La Franca F., Andreani P., Cristiani S., 1998, *ApJ*, 497, 529
- La Franca F., et al., 2005, *ApJ*, 635, 864
- La Franca F., et al., 2002, *ApJ*, 570, 100
- Lemson G., Virgo Consortium t., 2006, *ArXiv Astrophysics e-prints: 0608019*
- Lidz A., Hopkins P. F., Cox T. J., Hernquist L., Robertson B., 2006, *ApJ*, 641, 41
- Lopez J., DeGraf C., DiMatteo T., Fu B., Fink E., Gibson G., 2011, in *Statistical and Scientific Databases Management Conference (SSDBM)*, Portland, OR
- Magorrian J., et al., 1998, *AJ*, 115, 2285
- Makino J., Funato Y., 2004, *ApJ*, 602, 93
- Malbon R. K., Baugh C. M., Frenk C. S., Lacey C. G., 2007, *MNRAS*, 382, 1394
- Marulli F., Bonoli S., Branchini E., Gilli R., Moscardini L., Springel V., 2009, *MNRAS*, 396, 1404
- Marulli F., Bonoli S., Branchini E., Moscardini L., Springel V., 2008, *MNRAS*, 385, 1846
- Mayer L., Kazantzidis S., Madau P., Colpi M., Quinn T., Wadsley J., 2007, *Science*, 316, 1874
- Myers A. D., Brunner R. J., Nichol R. C., Richards G. T., Schneider D. P., Bahcall N. A., 2007, *ApJ*, 658, 85
- Pillepich A., Porciani C., Hahn O., 2010, *MNRAS*, 402, 191
- Porciani C., Magliocchetti M., Norberg P., 2004, *MNRAS*, 355, 1010
- Reed D. S., Bower R., Frenk C. S., Jenkins A., Theuns T., 2007, *MNRAS*, 374, 2
- Richards G. T., et al., 2005, *MNRAS*, 360, 839
- Richards G. T., et al., 2006, *AJ*, 131, 2766
- Ross N. P., et al., 2009, *ApJ*, 697, 1634
- Sazonov S. Y., Ostriker J. P., Sunyaev R. A., 2004, *MNRAS*, 347, 144
- Shakura N. I., Sunyaev R. A., 1973, *A&A*, 24, 337
- Shen Y., et al., 2007, *AJ*, 133, 2222
- Shen Y., et al., 2009, *ApJ*, 697, 1656
- Sheth R. K., Mo H. J., Tormen G., 2001, *MNRAS*, 323, 1

- Sijacki D., Springel V., di Matteo T., Hernquist L., 2007, MNRAS, 380, 877
- Sijacki D., Springel V., Haehnelt M. G., 2009, MNRAS, 400, 100
- Silverman J. D., et al., 2005, ApJ, 624, 630
- Silverman J. D., et al., 2008, ApJ, 679, 118
- Springel V., 2005, MNRAS, 364, 1105
- Springel V., Di Matteo T., Hernquist L., 2005a, MNRAS, 361, 776
- Springel V., Hernquist L., 2003, MNRAS, 339, 289
- Springel V., et al., 2005b, Nature, 435, 629
- Tinker J. L., Robertson B. E., Kravtsov A. V., Klypin A., Warren M. S., Yepes G., Gottlöber S., 2010, ApJ, 724, 878
- Tremaine S., et al., 2002, ApJ, 574, 740
- Ueda Y., Akiyama M., Ohta K., Miyaji T., 2003, ApJ, 598, 886
- Volonteri M., Haardt F., Madau P., 2003, ApJ, 582, 559
- Volonteri M., Rees M. J., 2006, ApJ, 650, 669
- Willott C. J., et al., 2010a, AJ, 140, 546
- Willott C. J., et al., 2010b, AJ, 139, 906
- Wyithe J. S. B., Loeb A., 2003, ApJ, 595, 614
- Yencho B., Barger A. J., Trouille L., Winter L. M., 2009, ApJ, 698, 380
- Yoshida N., Omukai K., Hernquist L., Abel T., 2006, ApJ, 652, 6
- Zheng Z., et al., 2005, ApJ, 633, 791